Connectivity-based parcellation of the anterior limb of the internal capsule

Pranav Nanda[1], **Garrett P. Banks**[1], **Yagna J. Pathak**[1], and **Sameer A. Sheth**[1,*]

[1]Columbia University Medical Center, Department of Neurological Surgery, New York, NY

Abstract

The anterior limb of internal capsule (ALIC) is an important locus of frontal-subcortical fiber tracts involved in cognitive and limbic feedback loops. However, the structural organization of its component fiber tracts remains unclear. Therefore, although the ALIC is a promising target for various neurosurgical procedures for psychiatric disorders, more precise understanding of its organization is required to optimize target localization. Using diffusion tensor imaging (DTI) collected on healthy subjects by the Human Connectome Project (HCP), we generated parcellations of the ALIC by dividing it according to structural connectivity to various frontal regions. We then compared individuals' parcellations in order to evaluate the ALIC's structural consistency. All 40 included subjects demonstrated a posterior-superior to anterior-inferior axis of tract organization in the ALIC. Nonetheless, subdivisions of the ALIC were found to vary substantially, as voxels in the average parcellation were accurately assigned for a mean of only 66.2% of subjects. There were, however, some loci of consistency, most notably in the region maximally connected to orbitofrontal cortex. These findings clarify the highly variable organization of the ALIC and may represent a tool for patient-specific targeting of neuromodulation.

1 Introduction

Frontal-subcortical cognitive and limbic feedback loops, which link prefrontal cortex to subcortical structures notably including the mediodorsal and anterior thalamic nuclei, modulate various higher cognitive functions, including attention, memory, emotional regulation, and sensory processing and gating [Bonelli and Cummings, 2007; Cummings, 1993; Lang et al., 2006; Levitt et al., 2002; Levy et al., 1997; Tekin and Cummings, 2002]. Connections between these prefrontal and subcortical regions course through white matter tracts within the anterior limb of the internal capsule (ALIC) [Albin et al., 1989; Alexander et al., 1991; Cummings, 1995; Levitt et al., 2010]. Abnormalities in the ALIC could therefore generate dysfunction in cognitive and limbic feedback loops, which could produce a wide variety of neuropsychiatric symptoms [Levitt et al., 2012].

Indeed, ALIC abnormalities have been observed in various psychiatric disorders, including schizophrenia, obsessive-compulsive disorder (OCD), and depression. For instance,

*Correspondence: Dr. Sameer A. Sheth, Department of Neurosurgery, Columbia University, 710 West 168th Street, Neurological Institute 435, New York, NY, 10032, USA. ss4451@cumc.columbia.edu.

reductions in ALIC volume have consistently been seen in studies of schizophrenia patients [Chua et al., 2007; Lang et al., 2006; Wobrock et al., 2008; Zhou et al., 2003]. Multiple diffusion tensor imaging (DTI) studies have also found that fractional anisotropy (FA) is abnormal in the ALIC of schizophrenia and OCD patients [Cannistraro et al., 2007; Jeong et al., 2009; Oh et al., 2009; Sussmann et al., 2009]. Abnormal FA is thought to be a marker of white matter integrity [Kochunov et al., 2007], but it may also indicate variable patterns of connectivity. Functional imaging studies suggest that, relative to controls, patients with OCD exhibit significantly increased metabolic activity at rest in various nodes of frontal-subcortical circuits, including orbitofrontal cortex (OFC), prefrontal cortex (PFC), and thalamus [Baxter et al., 1987; Baxter et al., 1988; Bourne et al., 2012; Göttlich et al., 2014; Saxena and Rauch, 2000; Saxena et al., 1998; Schwartz et al., 1996], and this increased metabolic activity appears to correlate with OCD symptomatology [Breiter et al., 1996; Göttlich et al., 2014; McGuire et al., 1994; Rauch et al., 1994; Schwartz et al., 1996; Simon et al., 2010]. Moreover, depression has been associated with macroscopic white matter lesions affecting frontal-subcortical feedback loops in patients suffering strokes [Vataja et al., 2001; Vataja et al., 2004].

Although the majority of patients with psychiatric disorders can be managed effectively by medical and behavioral therapies, stereotactic neurosurgical interventions are an important and useful option for those with severe, treatment-refractory disease [Nuttin et al., 2014]. Several of these neurosurgical procedures target the ALIC given its relevance in disease pathophysiology. For instance, anterior capsulotomy, a procedure pioneered by Talairach in 1949 [Talairach et al., 1949], demonstrates a 45–65% response rate for severe treatment refractory OCD [D'Astous et al., 2013; Kondziolka et al., 2011; Lopes et al., 2014; Rück et al., 2008; Sheehan et al., 2013]. Deep brain stimulation (DBS) of the ventral ALIC and adjacent ventral striatum (ventral capsule/ventral striatum, VC/VS) has also emerged as a treatment option for refractory OCD [Nuttin et al., 1999], and has exhibited response rate similar to that for capsulotomy [Abelson et al., 2005; Greenberg et al., 2008; Greenberg et al., 2006; Pepper et al., 2015; Roh et al., 2012; Tsai et al., 2012]. DBS of the VC/VS and surrounding region has also been explored as a potential therapy for treatment refractory depression [Gutman et al., 2009; Luyten et al., 2016; Malone et al., 2009]. However, precision is important in targeting these regions for neuromodulation, as modulation of nearby tracts, such as accumbens region outflow or PFC projections, may engender harmful side effects, such as panic or memory loss [Kooistra and Heilman, 1988; Scheibel and Scheibel, 1967; Shapira et al., 2006].

However, the precise locations of optimal neurosurgical targets within the ALIC remain uncertain as do the precise locations of functionally important but pathophysiologically unrelated tracts to be avoided, partially because neuroimaging work is still required to delineate the structural organization of involved circuits [Greenberg et al., 2010]. For example, with more experience, the DBS target for OCD has migrated to become increasingly posterior, approaching the junction of the ALIC, anterior commissure, and posterior ventral striatum [Greenberg et al., 2008]. The ALIC is thought to contain multiple frontal-subcortical circuits that underpin distinct behavioral functions [Bonelli and Cummings, 2007; Cummings, 1993; Levitt et al., 2010], although the organization of these circuits within the ALIC remains unclear. Rhesus monkey tract-tracing studies and initial

human tractography focusing on ventromedial prefrontal cortex suggest an organization of tracts along a dorsal-ventral gradient [Jbabdi et al., 2013; Schmahmann and Pandya, 2006]. Further clarification is required for tracts connecting with a broader range of prefrontal cortex. It would also be useful to understand how the organization of the ALIC differs between individuals, as there have been indications of inter-individual variability in prior research [Jbabdi et al., 2013]. Observing a high degree of variability could lend support for implementing more robust protocols for patient-specific targeting of neurosurgical procedures.

We therefore performed and compared different tractographic techniques on high-quality diffusion tensor imaging of healthy subjects in order to parcellate the ALIC by patterns of frontal connectivity. We then compared the ALIC parcellations between individuals in order to evaluate for patterns of consistency in the structural organization of prefrontal-subcortical tracts.

2 Materials and methods

2.1 Template-based parcellation

Frontothalamic radiations were generated using deterministic tractography on a template incorporating diffusion data from 842 Human Connectome Project controls (470 women, 372 men; 176 age 22–25, 367 age 26–30, 293 age 31–35, 6 age >36) with analysis performed in DSI Studio [Yeh and Tseng, 2011; Yeh et al., 2010]. For each hemisphere, tracts were developed by seeding from the ipsilateral thalamus (defined by the Harvard-Oxford subcortical atlas [Desikan et al., 2006]), using the ipsilateral ALIC (defined by the Johns Hopkins University white matter atlas [Hua et al., 2008]) as a waypoint, using the contralateral hemisphere as a region of avoidance, and using frontal Brodmann areas (BA04, BA06, BA08, BA09, BA10, BA11, BA44, BA45, BA46, and BA47) as independent terminating regions (Figure 1a). For each frontal Brodmann area (BA), 100,000 seeds were used on each side, and tractography parameters included a maximum turning angle of 50 degrees, minimum fractional anisotropy of 0.15, step size of 0.50mm, minimum length of 30mm, and maximum length of 300mm. Connections were only found to BA06 (supplementary motor area), BA08 (frontal eye fields), BA09 (medial and dorsolateral prefrontal cortex), BA10 (rostral prefrontal cortex), BA11 (orbitofrontal cortex), BA46 (dorsolateral prefrontal cortex), and BA47 (pars orbitalis), and so they were the only frontal BAs used for further analyses (Figure 1b). Tract densities within the ALIC were saved on the 1mm MNI152 template and normalized by dividing the volume of the corresponding individual frontal BAs, as calculated using the FMRIB Software Library v5.0 (FSL) [Jenkinson et al., 2012]. The ALIC was then parcellated using FSL by assigning each ALIC voxel to the frontal BA with maximum normalized tract density. A specificity index was calculated for each voxel of this template-based parcellation by dividing the maximum normalized tract density in this specific voxel by the voxel's total normalized tract density. For each voxel, the specificity index represented the maximum proportion of passing fibers going to the same frontal BA.

2.2 Individual-based parcellations

Parcellations were also generated on 40 randomly selected HCP subjects (22 women, 18 men; 4 age 22–25, 16 age 26–30, 20 age 31–35; Supplementary Table 1) in order to validate the findings of the template-based parcellation. HCP DTI data were prepared by modeling crossing fibers with up to three fibers per voxel using FMRIB's Diffusion Toolbox (FDT) [Behrens et al., 2007].

2.2.1 Probabilistic individual-based parcellation—Probabilistic parcellation was performed on each of the 40 subjects using connectivity-based seed classification in FDT [Behrens et al., 2003; Johansen-Berg et al., 2004]. For each hemisphere, voxels within the ipsilateral ALIC were used as seed regions and frontal BAs were used as target masks. The contralateral hemisphere and the ipsilateral basal ganglia, thalamus, and posterior limb of the interior capsule were used as regions of avoidance in order to eliminate anatomically invalid streamlines between the ALIC and included frontal regions (Supplementary Figure 1). Default tracking parameters were employed, including 5000 samples, 2000 steps, a curvature threshold of 0.2, and a step length of 0.50mm. The resulting parcellations were then non-linearly transformed into standard 1mm MNI152 space to enable comparison across individuals.

The 40 transformed probabilistic individual-based parcellations were consolidated into a single combined parcellation in winner-take-all fashion by assigning each ALIC voxel to the frontal BA with which it was most frequently associated in the 40 individual parcellations. For each ALIC voxel, the proportion of individuals whose parcellations matched the combined parcellation was calculated in order to assess the degree of consistency in ALIC organization. The combined parcellation was then thresholded four times so that it was restricted to voxels that were representative for at least 50%, 80%, 90%, or 100% of individuals. The volumes of ALIC regions associated with each included frontal BA were quantified for the combined parcellation and its thresholded versions.

2.2.2 Deterministic individual-based parcellation—A combined deterministic individual-based parcellation was also generated in order to isolate the source of differences between the deterministic template-based parcellation and the combined probabilistic individual-based parcellation. For this effort, individual-based parcellations were created for each of the 40 subjects using the same deterministic tractography techniques employed to create the template-based parcellation. As with the probabilistic individual-based parcellations, the 40 deterministic individual-based parcellations were non-linearly transformed into standard 1mm MNI152 space and were amalgamated in a winner-take-all fashion to produce a combined parcellation. The representativeness and consistency of this combined parcellation was also evaluated using the same methods of calculation and thresholding.

2.3 Comparisons between parcellations

The template-based parcellation, the combined probabilistic individual-based parcellation, and the combined deterministic individual-based parcellation were quantitatively compared to one another using the Sørensen-Dice index of similarity [Dice, 1945; Sørensen, 1948].

This index can be used to evaluate the spatial similarity of two regions by calculating the volume of their intersection divided by the average of their volumes. Essentially, it represents the overlapping fraction of two regions. When assessing the similarity of regions A and B, the index is calculated as 2|A∩B|/(|A|+|B|). Parcellations were compared in a pairwise fashion, one frontal BA at a time. For each frontal BA, a pair of parcellations was compared by calculating the Sørensen-Dice index for the regions in the parcellations corresponding to the selected Brodmann area. Similarly, probabilistic and deterministic individual-based parcellations for all 40 HCP subjects were compared pairwise to one another and to the template-based parcellation by calculating Sørensen-Dice indices for each frontal BA region.

3 Results

3.1 Template-based parcellation

The template-based parcellation technique yielded a 3235 mm^3 parcellation primarily covering the medial aspect of the ALIC (Figure 2a). ALIC regions associated with different frontal BAs were organized along a posterior-superior to anterior-inferior axis. The parcellation's most commonly represented BAs by volume were those associated with prefrontal cortex (PFC), namely BA09 and BA10 (Table 1). The mean (+/− standard deviation) specificity index (i.e., the proportion of streamlines passing through a voxel and terminating in the same frontal BA) was 0.882 +/− 0.171, and the median specificity index was 1.000 (Supplementary Figure 2).

3.2 Individual-based parcellations

All of the probabilistic and deterministic individual-based parcellations demonstrated a similar posterior-superior to anterior-inferior axis of organization (Figure 3; Supplementary Figure 3). However, unlike in the template-based parcellation, the medial aspects of subjects' probabilistic and deterministic individual-based parcellations were dominated by BA47 (Supplementary Figure 4; Supplementary Figure 5).

3.2.1 Probabilistic individual-based parcellation—The combined probabilistic individual-based parcellation spanned 6156 mm^3 covering the entire ALIC (Figure 2b). On average, the frontal BA assignments of voxels of the combined probabilistic parcellation were consistent with 66.2% (+/− 21.9%) of individuals' probabilistic parcellations (Figure 5; Supplementary Figure 6a). The region assigned to BA11 exhibited the highest degree of consistency across individuals, with 12.1% of the BA11 region of the combined probabilistic parcellation being assigned to BA11 in all 40 subjects (Table 1).

3.2.2 Deterministic individual-based parcellation—The combined deterministic individual-based parcellation covered 6153 mm^3 over the entire ALIC (Figure 2c). The deterministic parcellation was less consistently representative than the probabilistic parcellation, as the frontal BA assignments of voxels of the combined deterministic parcellation were consistent on average with 35.4% +/− 17.2% of subjects' deterministic parcellations (Supplementary Figure 6b; Supplementary Figure 7). No voxels in the entire

combined deterministic individual-based parcellation were consistently assigned across all 40 subjects (Table 1).

3.3 Comparisons between parcellations

The Sørensen-Dice indices of similarity between regions of the template-based and the probabilistic individual-based parcellations was 0.259 +/− 0.183 (Supplementary Figure 8a). The probabilistic individual-based parcellations exhibited greater similarity to one another, as the mean Sørensen-Dice index between probabilistic individual-based parcellation regions was 0.455 +/− 0.272 (Supplementary Figure 8b). Regions assigned to BA11 were the most similar to one another across probabilistic individual-based parcellations, with a mean Sørensen-Dice index of 0.714 +/− 0.076.

The Sørensen-Dice indices of similarity between regions of the template-based and the deterministic individual-based parcellations was 0.208 +/− 0.167 (Supplementary Figure 8c). The deterministic individual-based parcellations were less similar to one another than the probabilistic individual-based parcellations, as the mean Sørensen-Dice index between deterministic individual-based parcellation regions was 0.214 +/− 0.206 (Supplementary Figure 8d).

In comparing the summary parcellations to one another, the mean Sørensen-Dice index was 0.576 +/− 0.396 for the combined probabilistic and combined deterministic individual-based parcellations, 0.283 +/− 0.229 for the template-based and combined probabilistic individual-based parcellations, and 0.255 +/− 0.212 for the template-based and combined deterministic individual-based parcellations (Table 2).

4 Discussion

Our results illustrate the organization of the human ALIC based on its structural connectivity to different regions of the prefrontal cortex. Specifically, they reveal a posterior-superior to anterior-inferior axis of organization (Figure 2), which was found in all 40 subjects whose ALICs were parcellated individually. This axis runs parallel to the ALIC organization previously described in rhesus monkey tract-tracing studies [Schmahmann and Pandya, 2006] and to the dorsal-ventral gradient described in prior human tractographic studies [Jbabdi et al., 2013].

Although the general gestalt of ALIC organization was found to be consistent across all 40 subjects, there were still substantial organizational deviations between subjects. For instance, even for the probabilistic individual-based parcellations, which exhibited the least inter-subject variability, the mean Sørensen-Dice index for pairwise comparisons (0.455) suggested that, on average, less than half of the region assigned to the same frontal BA was shared between two individuals. Furthermore, voxels of the combined probabilistic individual-based parcellations were accurate for only a mean of 66.2% of subjects, and only 18.8% of voxels were similarly assigned for at least 90% of subjects (Table 1; Figure 4). Taken together, these results indicate that the exact locations of particular tracts running through the ALIC vary substantially between individuals.

These findings have implications for the application of neurosurgical procedures of the ALIC. The generalized combined probabilistic parcellation may provide a map for where to target procedures intended to modulate circuits involving certain frontal regions that are thought to be involved with disease neuropathophysiology (e.g., cortico-striato-thalamo-cortical circuits in OCD). Perhaps more pertinently, though, the high variability found in the ALIC suggests that the locations of optimal nodes to modulate these networks likely vary from patient to patient. The results of these analyses may therefore argue for taking a "precision medicine" approach to neuromodulation by performing preoperative tractography in order to develop patient-specific parcellations that inform patient-specific targeting.

It is notable that there is relative consistency across subjects in the location of the region of the ALIC predominantly connecting with BA11 (OFC), which is particularly targeted in capsulotomy and DBS for OCD [Greenberg et al., 2010]. This relative consistency of location may account for the high efficacy and response rates (approximately 55%) seen in these procedures [Greenberg et al., 2008; Lévêque et al., 2013]. It is possible that the relative consistency of the BA11 region may be partially attributed to its location at the ventral extreme of the ALIC, so that it only shows variability on the dorsal front. The consistency of the BA11 within healthy controls may also make it a useful reference point in comparisons between healthy individuals and patients. However, even this region of the ALIC exhibits some variation between healthy subjects. The voxels assigned to BA11 in the combined probabilistic parcellation were not assigned to BA11 for a mean of 26.6% of subjects' individual probabilistic parcellations (Supplementary Figure 5). Given that this region of the ALIC also exhibits substantial inconsistency between individuals, albeit less so than other ALIC regions, related procedures may still benefit from targeting that is informed by patient-specific tractography. Indeed, this anatomical inconsistency may account for a significant portion of the remaining variability in patient response following these procedures.

These results may also have methodological implications about the application of template-based versus individual-based approaches and the use of probabilistic or deterministic tractography. The template-based and individual-based parcellations showed similar general organizations, as they both had the same axis of orientation. However, the template-based parcellation did exhibit substantial qualitative differences (e.g., restriction of tracts to the medial aspect of the ALIC) and quantitative differences (e.g., average Sørensen-Dice indices less than 0.283 compared to the combined individual-based probabilistic and deterministic parcellations). It is possible that averaging diffusion data across subjects to create a template may wash out the effects of multimodal tensor distributions, which would lead to decreased tract sensitivity and accuracy. Findings based on template datasets should therefore be validated by individual-based analyses. Also, although the combined individual-based probabilistic and deterministic parcellations were fairly similar (Figure 2b; Figure 2c), the deterministic individual-based parcellations were far more variable (Table 2; Supplementary Figure 5). For instance, no voxels were consistently assigned across all 40 deterministic parcellations whereas 239 voxels were consistently assigned across all 40 probabilistic parcellations (Table 1). This finding of decreased consistency in deterministic parcellations could at least partially be explained by a decreased signal-to-noise ratio in the deterministic tractography methods used here.

These findings may be limited by the subdivision of the frontal lobe by BAs. Although this method was readily standardized and replicable across subjects, BAs are based on cytoarchitectural organization and so they may not perfectly delineate the functions of the frontal lobe, which may reduce the direct applicability of the developed ALIC parcellation. Also, although winner-takes-all classification generates discrete and interpretable parcellations, some information may be lost by this methodology. For instance, although a voxel may be dominated by connections to one frontal BA, it may also contain substantial connections to another, which are discarded in winner-takes-all parcellation.

Since white matter architecture has been shown to evolve [Lebel et al., 2012; Scholz et al., 2009], the ALIC organization described here may be representative of a state biological marker, but longitudinal studies would clarify whether it changes over time. To extend the implications of this study, it would be helpful to identify clinical and behavioral correlates of ALIC organization, both within pathologic and non-pathologic populations. It would also be useful to compare the ALIC organizations of healthy controls and patients. Analysis of the patient ALIC could both inform neurosurgical targeting and potentially clarify pathophysiology. Future investigations should correlate the localizations of neurosurgical procedures as per ALIC parcellation with patient outcomes and anatomic or functional changes, as can be measured by modalities like structural imaging, functional imaging, or EEG. Doing so might elucidate the mechanisms and consequences of neuromodulation.

5 Conclusion

Overall, the findings here describe the organization of the human ALIC, an important and clinically relevant white matter region. Specifically, they describe a consistent posterior-superior to anterior-inferior axis of organization. However, they also underscore the high degree of variability between individuals' patterns of frontal structural connectivity within the ALIC. This study may therefore represent a step towards prospectively performing patient-specific tractography and parcellation in order to inform and optimize the targeting for neurosurgical procedures focused on this region.

Supplementary Material

Refer to Web version on PubMed Central for supplementary material.

Acknowledgments

References

Abelson JL, Curtis GC, Sagher O, Albucher RC, Harrigan M, Taylor SF, Martis B, Giordani B. Deep brain stimulation for refractory obsessive-compulsive disorder. Biol Psychiatry. 2005; 57:510–516. [PubMed: 15737666]

Albin RL, Young AB, Penney JB. The functional anatomy of basal ganglia disorders. Trends Neurosci. 1989; 12:366–375. [PubMed: 2479133]

Alexander GE, Crutcher MD, DeLong MR. Basal ganglia-thalamocortical circuits: Parallel substrates for motor, oculomotor, "prefrontal" and 'limbic' functions. Progress in Brain Research. 1991; 85:119–146.

Baxter LR, Phelps ME, Mazziotta JC, Guze BH, Schwartz JM, Selin CE. Local cerebral glucose metabolic rates in obsessive-compulsive disorder. A comparison with rates in unipolar depression and in normal controls. Arch Gen Psychiatry. 1987; 44:211–218. [PubMed: 3493749]

Baxter LR, Schwartz JM, Mazziotta JC, Phelps ME, Pahl JJ, Guze BH, Fairbanks L. Cerebral glucose metabolic rates in nondepressed patients with obsessive-compulsive disorder. Am J Psychiatry. 1988; 145:1560–1563. [PubMed: 3264118]

Behrens TEJ, Berg HJ, Jbabdi S, Rushworth MFS, Woolrich MW. Probabilistic diffusion tractography with multiple fibre orientations: What can we gain? NeuroImage. 2007; 34:144–155. [PubMed: 17070705]

Behrens TEJ, Johansen-Berg H, Woolrich MW, Smith SM, Wheeler-Kingshott CAM, Boulby PA, Barker GJ, Sillery EL, Sheehan K, Ciccarelli O, Thompson AJ, Brady JM, Matthews PM. Non-invasive mapping of connections between human thalamus and cortex using diffusion imaging. Nat Neurosci. 2003; 6:750–757. [PubMed: 12808459]

Bonelli RM, Cummings JL. Frontal-subcortical circuitry and behavior. Dialogues Clin Neurosci. 2007; 9:141–151. [PubMed: 17726913]

Bourne SK, Eckhardt CA, Sheth SA, Eskandar EN. Mechanisms of deep brain stimulation for obsessive compulsive disorder: effects upon cells and circuits. Front Integr Neurosci. 2012; 6:29. [PubMed: 22712007]

Breiter HC, Rauch SL, Kwong KK, Baker JR, Weisskoff RM, Kennedy DN, Kendrick AD, Davis TL, Jiang A, Cohen MS, Stern CE, Belliveau JW, Baer L, O'Sullivan RL, Savage CR, Jenike MA, Rosen BR. Functional magnetic resonance imaging of symptom provocation in obsessive-compulsive disorder. Arch Gen Psychiatry. 1996; 53:595–606. [PubMed: 8660126]

Cannistraro PA, Makris N, Howard JD, Wedig MM, Hodge SM, Wilhelm S, Kennedy DN, Rauch SL. A diffusion tensor imaging study of white matter in obsessive–compulsive disorder. Depression and Anxiety. 2007; 24:440–446. [PubMed: 17096398]

Chua SE, Cheung C, Cheung V, Tsang JTK, Chen EYH, Wong JCH, Cheung JPY, Yip L, Tai K-S, Suckling J, McAlonan GM. Cerebral grey, white matter and csf in never-medicated, first-episode schizophrenia. Schizophrenia Research. 2007; 89:12–21. [PubMed: 17098398]

Cummings JL. Frontal-subcortical circuits and human behavior. Arch Neurol. 1993; 50:873–880. [PubMed: 8352676]

Cummings JL. Anatomic and behavioral aspects of frontal-subcortical circuits. Ann N Y Acad Sci. 1995; 769:1–13.

D'Astous M, Cottin S, Roy M, Picard C, Cantin L. Bilateral stereotactic anterior capsulotomy for obsessive-compulsive disorder: long-term follow-up. J Neurol Neurosurg Psychiatr. 2013; 84:1208–1213.

Desikan RS, Ségonne F, Fischl B, Quinn BT, Dickerson BC, Blacker D, Buckner RL, Dale AM, Maguire RP, Hyman BT, Albert MS, Killiany RJ. An automated labeling system for subdividing the human cerebral cortex on MRI scans into gyral based regions of interest. NeuroImage. 2006; 31:968–980. [PubMed: 16530430]

Dice LR. Measures of the Amount of Ecologic Association Between Species. Ecology. 1945; 26:297–302.

Göttlich M, Krämer UM, Kordon A, Hohagen F, Zurowski B. Decreased limbic and increased fronto-parietal connectivity in unmedicated patients with obsessive-compulsive disorder. Hum Brain Mapp. 2014; 35:5617–5632. [PubMed: 25044747]

Greenberg BD, Gabriels LA, Malone DA, Rezai AR, Friehs GM, Okun MS, Shapira NA, Foote KD, Cosyns PR, Kubu CS, Malloy PF, Salloway SP, Giftakis JE, Rise MT, Machado AG, Baker KB, Stypulkowski PH, Goodman WK, Rasmussen SA, Nuttin BJ. Deep brain stimulation of the ventral internal capsule/ventral striatum for obsessive-compulsive disorder: worldwide experience. Mol Psychiatry. 2008; 15:64–79. [PubMed: 18490925]

Greenberg BD, Malone DA, Friehs GM, Rezai AR, Kubu CS, Malloy PF, Salloway SP, Okun MS, Goodman WK, Rasmussen SA. Three-year outcomes in deep brain stimulation for highly resistant obsessive-compulsive disorder. Neuropsychopharmacology. 2006; 31:2384–2393. [PubMed: 16855529]

Greenberg BD, Rauch SL, Haber SN. Invasive circuitry-based neurotherapeutics: stereotactic ablation and deep brain stimulation for OCD. Neuropsychopharmacology. 2010; 35:317–336. [PubMed: 19759530]

Gutman DA, Holtzheimer PE, Behrens TEJ, Johansen-Berg H, Mayberg HS. A tractography analysis of two deep brain stimulation white matter targets for depression. Biol Psychiatry. 2009; 65:276–282. [PubMed: 19013554]

Hua K, Zhang J, Wakana S, Jiang H, Li X, Reich DS, Calabresi PA, Pekar JJ, van Zijl PCM, Mori S. Tract probability maps in stereotaxic spaces: analyses of white matter anatomy and tract-specific quantification. NeuroImage. 2008; 39:336–347. [PubMed: 17931890]

Jbabdi S, Lehman JF, Haber SN, Behrens TE. Human and monkey ventral prefrontal fibers use the same organizational principles to reach their targets: tracing versus tractography. J Neurosci. 2013; 33:3190–3201. [PubMed: 23407972]

Jenkinson M, Beckmann CF, Behrens TEJ, Woolrich MW, Smith SM. FSL. NeuroImage. 2012; 62:782–790. [PubMed: 21979382]

Jeong B, Wible CG, Hashimoto R-I, Kubicki M. Functional and anatomical connectivity abnormalities in left inferior frontal gyrus in schizophrenia. Hum Brain Mapp. 2009; 30:4138–4151. [PubMed: 19569073]

Johansen-Berg H, Behrens TEJ, Robson MD, Drobnjak I, Rushworth MFS, Brady JM, Smith SM, Higham DJ, Matthews PM. Changes in connectivity profiles define functionally distinct regions in human medial frontal cortex. Proceedings of the National Academy of Sciences of the United States of America. 2004; 101:13335–13340. [PubMed: 15340158]

Kochunov P, Thompson PM, Lancaster JL, Bartzokis G, Smith S, Coyle T, Royall DR, Laird A, Fox PT. Relationship between white matter fractional anisotropy and other indices of cerebral health in normal aging: tract-based spatial statistics study of aging. NeuroImage. 2007; 35:478–487. [PubMed: 17292629]

Kondziolka D, Flickinger JC, Hudak R. Results following gamma knife radiosurgical anterior capsulotomies for obsessive compulsive disorder. Neurosurgery. 2011; 68:28–32. [PubMed: 21150752]

Kooistra CA, Heilman KM. Memory loss from a subcortical white matter infarct. J Neurol Neurosurg Psychiatr. 1988; 51:866–869.

Lang DJ, Khorram B, Goghari VM, Kopala LC, Vandorpe RA, Rui Q, Smith GN, Honer WG. Reduced anterior internal capsule and thalamic volumes in first-episode psychosis. Schizophrenia Research. 2006; 87:89–99. [PubMed: 16793239]

Lebel C, Gee M, Camicioli R, Wieler M, Martin W, Beaulieu C. Diffusion tensor imaging of white matter tract evolution over the lifespan. NeuroImage. 2012; 60:340–352. [PubMed: 22178809]

Levitt JJ, Alvarado JL, Nestor PG, Rosow L, Pelavin PE, McCarley RW, Kubicki M, Shenton ME. Fractional anisotropy and radial diffusivity: diffusion measures of white matter abnormalities in the anterior limb of the internal capsule in schizophrenia. Schizophrenia Research. 2012; 136:55–62. [PubMed: 22019073]

Levitt JJ, Kubicki M, Nestor PG, Ersner-Hershfield H, Westin C-F, Alvarado JL, Kikinis R, Jolesz FA, McCarley RW, Shenton ME. A diffusion tensor imaging study of the anterior limb of the internal capsule in schizophrenia. Psychiatry Res. 2010; 184:143–150. [PubMed: 21055906]

Levitt JJ, McCarley RW, Dickey CC, Voglmaier MM, Niznikiewicz MA, Seidman LJ, Hirayasu Y, Ciszewski AA, Kikinis R, Jolesz FA, Shenton ME. MRI study of caudate nucleus volume and its cognitive correlates in neuroleptic-naive patients with schizotypal personality disorder. Am J Psychiatry. 2002; 159:1190–1197. [PubMed: 12091198]

Levy R, Friedman HR, Davachi L, Goldman-Rakic PS. Differential activation of the caudate nucleus in primates performing spatial and nonspatial working memory tasks. J Neurosci. 1997; 17:3870–3882. [PubMed: 9133405]

Lévêque M, Carron R, Régis J. Radiosurgery for the treatment of psychiatric disorders: a review. World Neurosurg. 2013; 80:S32e1–9.

Lopes AC, Greenberg BD, Canteras MM, Batistuzzo MC, Hoexter MQ, Gentil AF, Pereira CAB, Joaquim MA, de Mathis ME, D'Alcante CC, Taub A, de Castro DG, Tokeshi L, Sampaio LANPC, Leite CC, Shavitt RG, Diniz JB, Busatto G, Norén G, Rasmussen SA, Miguel EC. Gamma ventral capsulotomy for obsessive-compulsive disorder: a randomized clinical trial. JAMA Psychiatry. 2014; 71:1066–1076. [PubMed: 25054836]

Luyten L, Hendrickx S, Raymaekers S, Gabriëls L, Nuttin B. Electrical stimulation in the bed nucleus of the stria terminalis alleviates severe obsessive-compulsive disorder. Mol Psychiatry. 2016; 21:1272–1280. [PubMed: 26303665]

Malone DA, Dougherty DD, Rezai AR, Carpenter LL, Friehs GM, Eskandar EN, Rauch SL, Rasmussen SA, Machado AG, Kubu CS, Tyrka AR, Price LH, Stypulkowski PH, Giftakis JE, Rise MT, Malloy PF, Salloway SP, Greenberg BD. Deep brain stimulation of the ventral capsule/ventral striatum for treatment-resistant depression. Biol Psychiatry. 2009; 65:267–275. [PubMed: 18842257]

McGuire PK, Bench CJ, Frith CD, Marks IM, Frackowiak RS, Dolan RJ. Functional anatomy of obsessive-compulsive phenomena. The British Journal of Psychiatry. 1994; 164:459–468. [PubMed: 8038933]

Nuttin B, Cosyns P, Demeulemeester H, Gybels J, Meyerson B. Electrical stimulation in anterior limbs of internal capsules in patients with obsessive-compulsive disorder. Lancet. 1999; 354:1526.

Nuttin B, Wu H, Mayberg H, Hariz M, Gabriëls L, Galert T, Merkel R, Kubu C, Vilela-Filho O, Matthews K, Taira T, Lozano AM, Schechtmann G, Doshi P, Broggi G, Régis J, Alkhani A, Sun B, Eljamel S, Schulder M, Kaplitt M, Eskandar E, Rezai A, Krauss JK, Hilven P, Schuurman R, Ruiz P, Chang JW, Cosyns P, Lipsman N, Voges J, Cosgrove R, Li Y, Schlaepfer T. Consensus on guidelines for stereotactic neurosurgery for psychiatric disorders. Journal of neurology, neurosurgery, and psychiatry. 2014

Oh JS, Kubicki M, Rosenberger G, Bouix S, Levitt JJ, McCarley RW, Westin C-F, Shenton ME. Thalamo-frontal white matter alterations in chronic schizophrenia: a quantitative diffusion tractography study. Hum Brain Mapp. 2009; 30:3812–3825. [PubMed: 19449328]

Pepper J, Hariz M, Zrinzo L. Deep brain stimulation versus anterior capsulotomy for obsessive-compulsive disorder: a review of the literature. J Neurosurg. 2015; 122:1028–1037. [PubMed: 25635480]

Rauch SL, Jenike MA, Alpert NM, Baer L, Breiter HC, Savage CR, Fischman AJ. Regional cerebral blood flow measured during symptom provocation in obsessive-compulsive disorder using oxygen 15-labeled carbon dioxide and positron emission tomography. Arch Gen Psychiatry. 1994; 51:62–70. [PubMed: 8279930]

Roh D, Chang WS, Chang JW, Kim C-H. Long-term follow-up of deep brain stimulation for refractory obsessive-compulsive disorder. Psychiatry Res. 2012; 200:1067–1070. [PubMed: 22784468]

Rück C, Karlsson A, Steele JD, Edman G, Meyerson BA, Ericson K, Nyman H, Asberg M, Svanborg P. Capsulotomy for obsessive-compulsive disorder: long-term follow-up of 25 patients. Arch Gen Psychiatry. 2008; 65:914–921. [PubMed: 18678796]

Saxena S, Brody AL, Schwartz JM, Baxter LR. Neuroimaging and frontal-subcortical circuitry in obsessive-compulsive disorder. Br J Psychiatry Suppl. 1998:26–37.

Saxena S, Rauch SL. Functional neuroimaging and the neuroanatomy of obsessive-compulsive disorder. Psychiatr Clin North Am. 2000; 23:563–586. [PubMed: 10986728]

Scheibel ME, Scheibel AB. Structural organization of nonspecific thalamic nuclei and their projection toward cortex. Brain Res. 1967; 6:60–94. [PubMed: 4964024]

Schmahmann JD, Pandya DN. Internal Capsule. In: Schmahmann JD, Pandya DN, editorsFiber Pathways of the Brain. Oxford: Oxford University Press; 2006.

Scholz J, Klein MC, Behrens TEJ, Johansen-Berg H. Training induces changes in white-matter architecture. Nat Neurosci. 2009; 12:1370–1371. [PubMed: 19820707]

Schwartz JM, Stoessel PW, Baxter LR, Martin KM, Phelps ME. Systematic changes in cerebral glucose metabolic rate after successful behavior modification treatment of obsessive-compulsive disorder. Arch Gen Psychiatry. 1996; 53:109–113. [PubMed: 8629886]

Shapira NA, Okun MS, Wint D, Foote KD, Byars JA, Bowers D, Springer US, Lang PJ, Greenberg BD, Haber SN, Goodman WK. Panic and fear induced by deep brain stimulation. J Neurol Neurosurg Psychiatr. 2006; 77:410–412.

Sheehan JP, Patterson G, Schlesinger D, Xu Z. γ knife surgery anterior capsulotomy for severe and refractory obsessive-compulsive disorder. J Neurosurg. 2013; 119:1112–1118. [PubMed: 23829816]

Simon D, Kaufmann C, Müsch K, Kischkel E, Kathmann N. Fronto-striato-limbic hyperactivation in obsessive-compulsive disorder during individually tailored symptom provocation. Psychophysiology. 2010; 47:728–738. [PubMed: 20158678]

Sussmann JE, Lymer GKS, McKirdy J, Moorhead TWJ, Muñoz Maniega S, Job D, Hall J, Bastin ME, Johnstone EC, Lawrie SM, McIntosh AM. White matter abnormalities in bipolar disorder and schizophrenia detected using diffusion tensor magnetic resonance imaging. Bipolar Disord. 2009; 11:11–18. [PubMed: 19133962]

Sørensen T. A method of establishing groups of equal amplitude in plant sociology based on similarity of species and its application to analyses of the vegetation on Danish commons. Kongelige Danske Videnskabernes Selskab. 1948; 5:1–34.

Talairach J, Hecaen H, David M. Lobotomie prefrontale limitee par electrocoagulation des fibres thalamo-frontalis leur emergence du bras anterior de la capsule interne. Paris. Proceedings of the 4th Congress Neurologique Internationale; 1949. 141

Tekin S, Cummings JL. Frontal–subcortical neuronal circuits and clinical neuropsychiatry: An update. Journal of Psychosomatic Research. 2002; 53:647–654. [PubMed: 12169339]

Tsai H-C, Chang C-H, Pan J-I, Hsieh H-J, Tsai S-T, Hung H-Y, Chen S-Y. Pilot study of deep brain stimulation in refractory obsessive-compulsive disorder ethnic Chinese patients. Psychiatry Clin Neurosci. 2012; 66:303–312. [PubMed: 22624735]

Vataja R, Leppävuori A, Pohjasvaara T, Mäntylä R, Aronen HJ, Salonen O, Kaste M, Erkinjuntti T. Poststroke depression and lesion location revisited. J Neuropsychiatry Clin Neurosci. 2004; 16:156–162. [PubMed: 15260366]

Vataja R, Pohjasvaara T, Leppävuori A, Mäntylä R, Aronen HJ, Salonen O, Kaste M, Erkinjuntti T. Magnetic resonance imaging correlates of depression after ischemic stroke. Arch Gen Psychiatry. 2001; 58:925–931. [PubMed: 11576030]

Wobrock T, Kamer T, Roy A, Vogeley K, Schneider-Axmann T, Wagner M, Maier W, Rietschel M, Schulze TG, Scherk H, Schild HH, Block W, Träber F, Tepest R, Honer WG, Falkai P. Reduction of the internal capsule in families affected with schizophrenia. Biol Psychiatry. 2008; 63:65–71. [PubMed: 17574215]

Yeh F-C, Tseng W-YI. NTU-90: a high angular resolution brain atlas constructed by q-space diffeomorphic reconstruction. NeuroImage. 2011; 58:91–99. [PubMed: 21704171]

Yeh F-C, Wedeen VJ, Tseng W-YI. Generalized q-sampling imaging. IEEE Trans Med Imaging. 2010; 29:1626–1635. [PubMed: 20304721]

Zhou S-Y, Suzuki M, Hagino H, Takahashi T, Kawasaki Y, Nohara S, Yamashita I, Seto H, Kurachi M. Decreased volume and increased asymmetry of the anterior limb of the internal capsule in patients with schizophrenia. Biol Psychiatry. 2003; 54:427–436. [PubMed: 12915287]
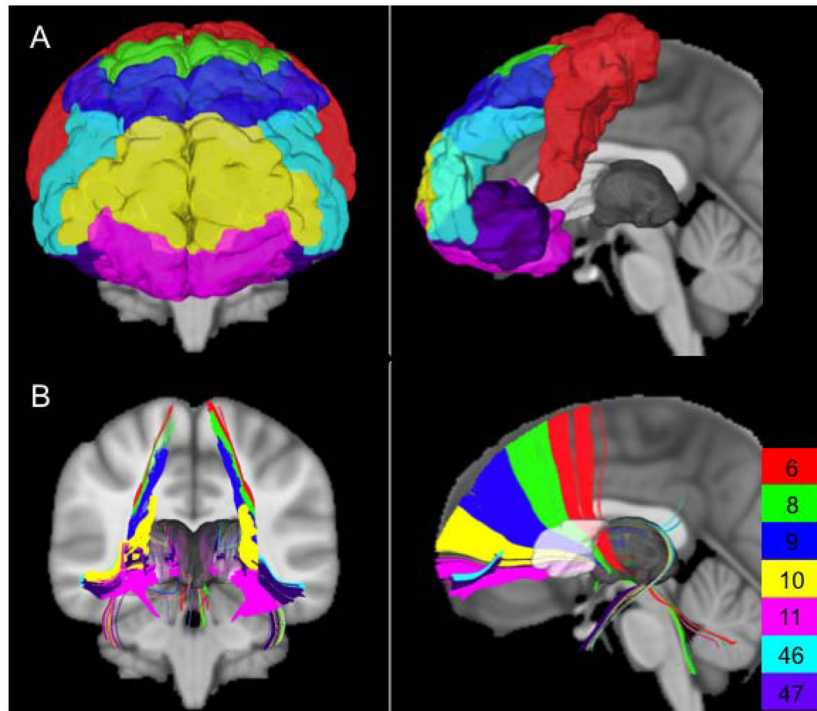
Figure 1. Included frontal Brodmann areas and corresponding frontothalamic radiations
(A) The frontal BAs included in analyses and (B) the connections between the thalamus and these frontal BAs through the ALIC as generated by deterministic template-based tractography
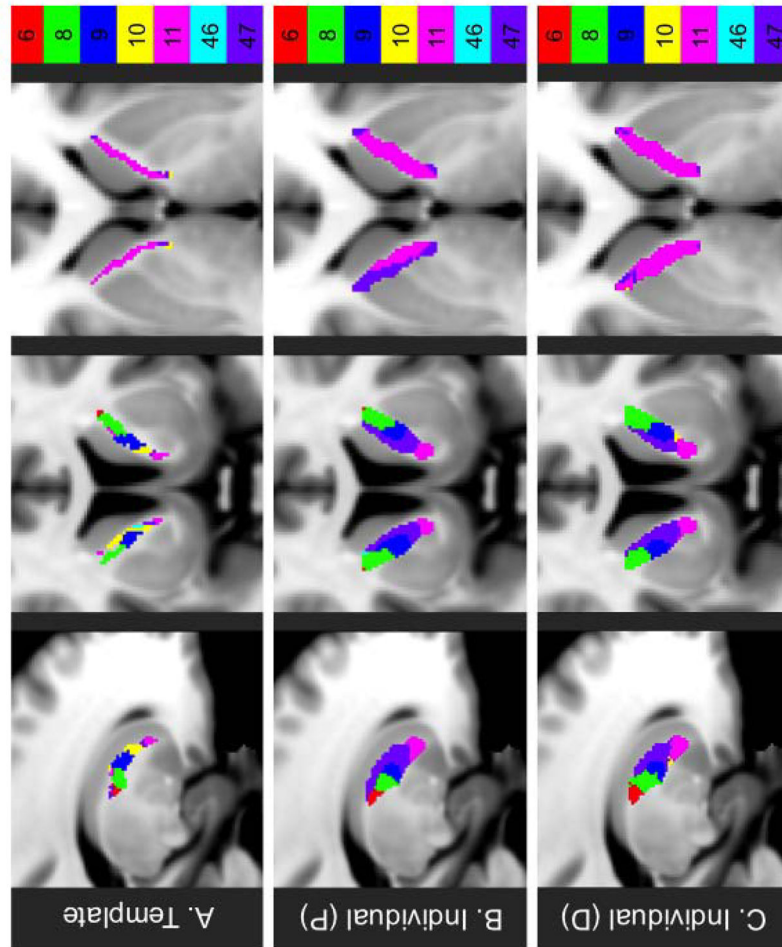
Figure 2. Parcellations of the ALIC

Mappings of the ALIC as generated by (A) deterministic template-based, (B) combined probabilistic individual-based, and (C) combined deterministic individual-based tractography
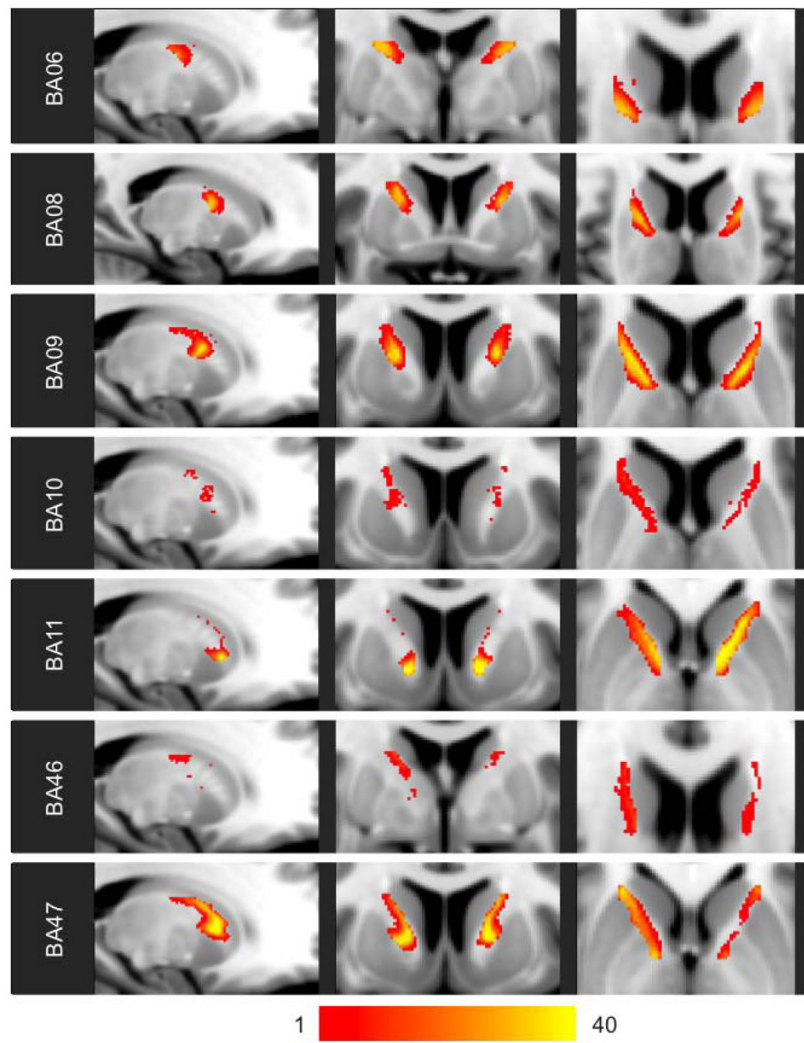
Figure 3. Heat maps of probabilistic individual-based parcellations
The color scale indicates the number of the 40 analyzed HCP subjects for whom probabilistic individual-based parcellation resulted in a voxel being assigned to the indicated frontal BA.
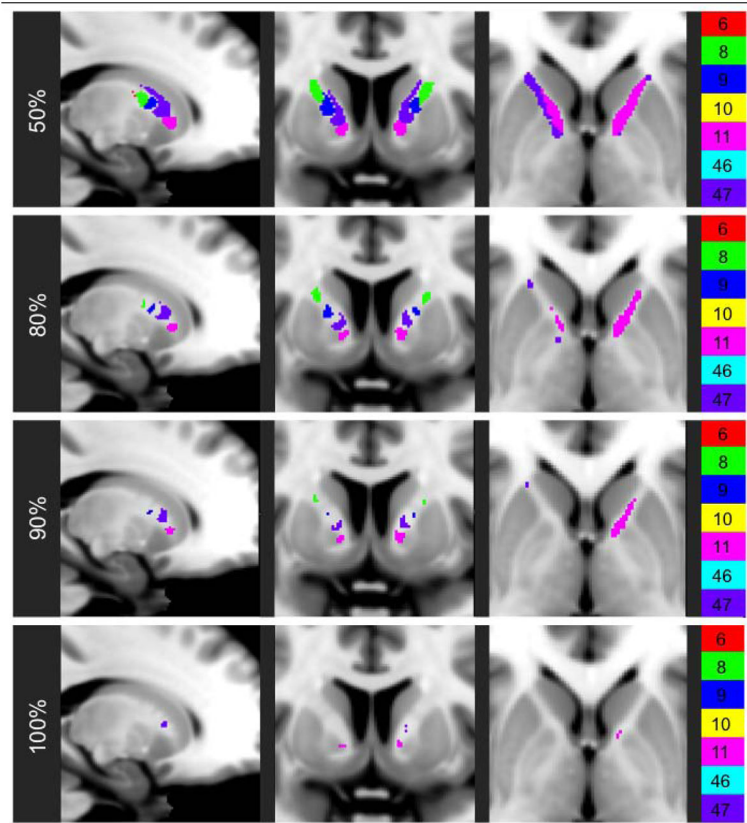
Figure 4. Combined probabilistic parcellation at varying thresholds of consistency
The voxels of the combined probabilistic individual-based parcellation that are assigned
accurately for at least the indicated percent of the analyzed HCP subjects

Table 1

Volumes of regions within parcellations

The table indicates the volumes of the ALIC subdivisions as per different parcellation techniques. The percentages shown in the individual-based columns represent the proportion of the ALIC subdivisions accurately assigned by the combined parcellation for at least the indicated percent of analyzed HCP subjects.

BA	Template Based	Combined Probabilistic Individual Based						Combined Deterministic Individual Based					
		Volume	50%	80%	90%	100%		Volume	50%	80%	90%	100%
BA06	236mm^3	555mm^3	76.0%	34.2%	19.6%	4.3%		452mm^3	33.8%	0.0%	0.0%	0.0%
BA08	561mm^3	907mm^3	76.3%	23.7%	5.5%	0.0%		1145mm^3	17.4%	0.0%	0.0%	0.0%
BA09	817mm^3	956mm^3	71.9%	22.9%	5.5%	0.0%		734mm^3	0.1%	0.0%	0.0%	0.0%
BA10	716mm^3	0mm^3	---	---	---	---		62mm^3	0.0%	0.0%	0.0%	0.0%
BA11	448mm^3	871mm^3	85.0%	49.6%	36.9%	12.1%		1067mm^3	22.6%	0.1%	0.0%	0.0%
BA46	75mm^3	73mm^3	0.0%	0.0%	0.0%	0.0%		1mm^3	0.0%	0.0%	0.0%	0.0%
BA47	382mm^3	2794mm^3	78.4%	37.9%	22.3%	3.9%		2692mm^3	33.6%	0.5%	0.0%	0.0%
Total	3235mm^3	6156mm^3	76.9%	34.3%	18.8%	3.9%		6153mm^3	24.4%	0.2%	0.0%	0.0%

Table 2

Sørensen-Dice indices comparing parcellations

This table indicates the Sørensen-Dice indices comparing both summary parcellations (template, T; combined probabilistic, P; and combined deterministic, D) and individual-based parcellations for each frontal BA region.

Region	Summary Comparisons			Individual Comparisons (mean/sd)	
	T-P	T-D	P-D	Probabilistic	Deterministic
BA06	0.493	0.456	0.824	0.603 (0.101)	0.351 (0.171)
BA08	0.523	0.523	0.803	0.549 (0.113)	0.291 (0.178)
BA09	0.305	0.221	0.714	0.484 (0.126)	0.139 (0.132)
BA10	0.000	0.000	0.000	0.056 (0.072)	0.030 (0.064)
BA11	0.482	0.399	0.853	0.698 (0.101)	0.324 (0.177)
BA46	0.000	0.000	0.000	0.072 (0.095)	0.003 (0.017)
BA47	0.177	0.185	0.836	0.656 (0.129)	0.370 (0.182)